Journal of Neuroimmunology 332 (2019) 176–186

Contents lists available at ScienceDirect

Journal of Neuroimmunology

journal homepage: www.elsevier.com/locate/jneuroim

VEGF- and PDGF-dependent proliferation of oligodendrocyte progenitor cells in the medulla oblongata after LPC-induced focal demyelination

Daishi Hiratsuka[a], Erkin Kurganov[a], Eriko Furube[a], Mitsuhiro Morita[b], Seiji Miyata[a,*]

[a] Department of Applied Biology, Kyoto Institute of Technology, Matsugasaki, Sakyo-ku, Kyoto 606-8585, Japan
[b] Department of Biology, Graduate School of Science, Kobe University, Kobe, 657-8501, Japan

ARTICLE INFO

Keywords:
Oligodendrogenesis
Myelin
Brain stem
Neural stem cell
Circumventricular organ

ABSTRACT

The myelin sheath is critical in maintaining normal functions of the adult central nervous system (CNS) and the loss of the myelin sheath results in various neurological diseases. Although remyelination is the intrinsic repair system against demyelination that new myelin sheath is formed around axons in the adult CNS, little has been reported on remyelination system in the medulla oblongata. In the present study, we showed that the proliferation of oligodendrocyte progenitor cells (OPCs) was increased in the medulla oblongata by lysophosphatidylcholine (LPC)-induced focal demyelination, but that of NSCs was not changed. The inhibition of vascular endothelial growth factor (VEGF)- and platelet-derived growth factor (PDGF)-signaling suppressed the proliferation of OPCs by LPC-induced demyelination. Thus, the present study indicates that resident OPCs contribute to focal remyelination and VEGF and PDGF signaling is required for the proliferation of OPCs in the medulla oblongata of the adult mouse.

1. Introduction

The myelin sheath is essential for supply of trophic substance to axons, speed up of action potential, and protection of axons from external damage in the central nervous system (CNS) (Dupree et al., 2004; Jafarzadeh and Nemati, 2018; Kaplan et al., 1997). Oligodendrocytes are well known as the myelin-forming cells in the CNS and essential for proper brain function (Edgar and Nave, 2009). Mature myelinating oligodendrocytes are continuously produced from resident oligodendrocyte precursor cells (OPCs) in the corpus callosum, striatum, and fornix of normal adult forebrain (Ffrench-Constant and Raff, 1986; Rivers et al., 2008). Moreover, neural stem cells (NSCs) in the subventricular zone (SVZ) represent an important endogenous source of OPCs for preserving a population of oligodendrocytes in the white matter of normal adult forebrain (Dimou et al., 2008; Menn et al., 2006; Nait-Oumesmar et al., 1999). After lysophosphatidylcholine (LPC)-induced focal demyelination, OPCs derived from NSCs in the SVZ produce new mature oligodendrocytes in the corpus callosum (Nait-Oumesmar et al., 1999) and resident OPCs can supply oligodendrocytes for myelin sheath repair in the subcortical white matter cinglum and corpus callosum (Gensert and Goldman, 1997).

Demyelinating diseases include a group of progressive disorders that are characterized by an extensive loss of oligodendrocytes and the myelin sheaths from axonal fibers. Multiple sclerosis (MS) is the most common demyelinating disease and defined as widespread loss of the myelin sheaths from axonal fibers (Franklin and Ffrench-Constant, 2008; Peterson and Fujinami, 2007). The proliferation of OPCs occurs in the patient of MS (Dubois-Dalcq et al., 2005; Nait-Oumesmar et al., 2007; Scolding et al., 1998) and experimental autoimmune encephalomyelitis (EAE), an animal model of MS (Girolamo et al., 2011; Guo et al., 2011; Picard-Riera et al., 2002). The SVZ is a source to generate OPCs and replace oligodendrocytes in the olfactory bulb and corpus callosum of EAE-induced mouse (Picard-Riera et al., 2002). The Dramatic proliferation of resident OPCs in the cerebral cortex occurs at

Abbreviations: AP, area postrema; APC, adenomatous polyposis coli; BrdU, bromodeoxyuridine; CC, central canal; EAE, experimental autoimmune encephalomyelitis; EGF, epidermal growth factor; EGFR, epidermal growth factor receptor; FGF-2, fibroblast growth factor-2; GFAP, glial fibrillary acidic protein; GFP, green fluorescent protein; 12 N, hypoglossal nucleus; Iba1, ionized calcium-binding adapter molecule 1; LPC, lysophosphatidylcholine; MBP, myelin basic protein; MRI, magnetic resonance imaging; MS, multiple sclerosis; NGS, normal goat serum; NSCs, neural stem cells; MOG, myelin oligodendrocyte glycoprotein; Olig2, oligodendrocyte transcription factor 2; OPCs, oligodendrocyte precursor cells; PBS, phosphate-buffered saline; PBST, PBS containing 0.3% Triton X-100; PDGF, platelet-derived growth factor; Sol, the nucleus of the solitary tract; SVZ, subventricular zone; SOX2, sex determining region Y-box 2; VEGF, vascular endothelial growth factor

* Corresponding author.
E-mail address: smiyata@kit.ac.jp (S. Miyata).

https://doi.org/10.1016/j.jneuroim.2019.04.016
Received 28 January 2019; Received in revised form 28 April 2019; Accepted 29 April 2019

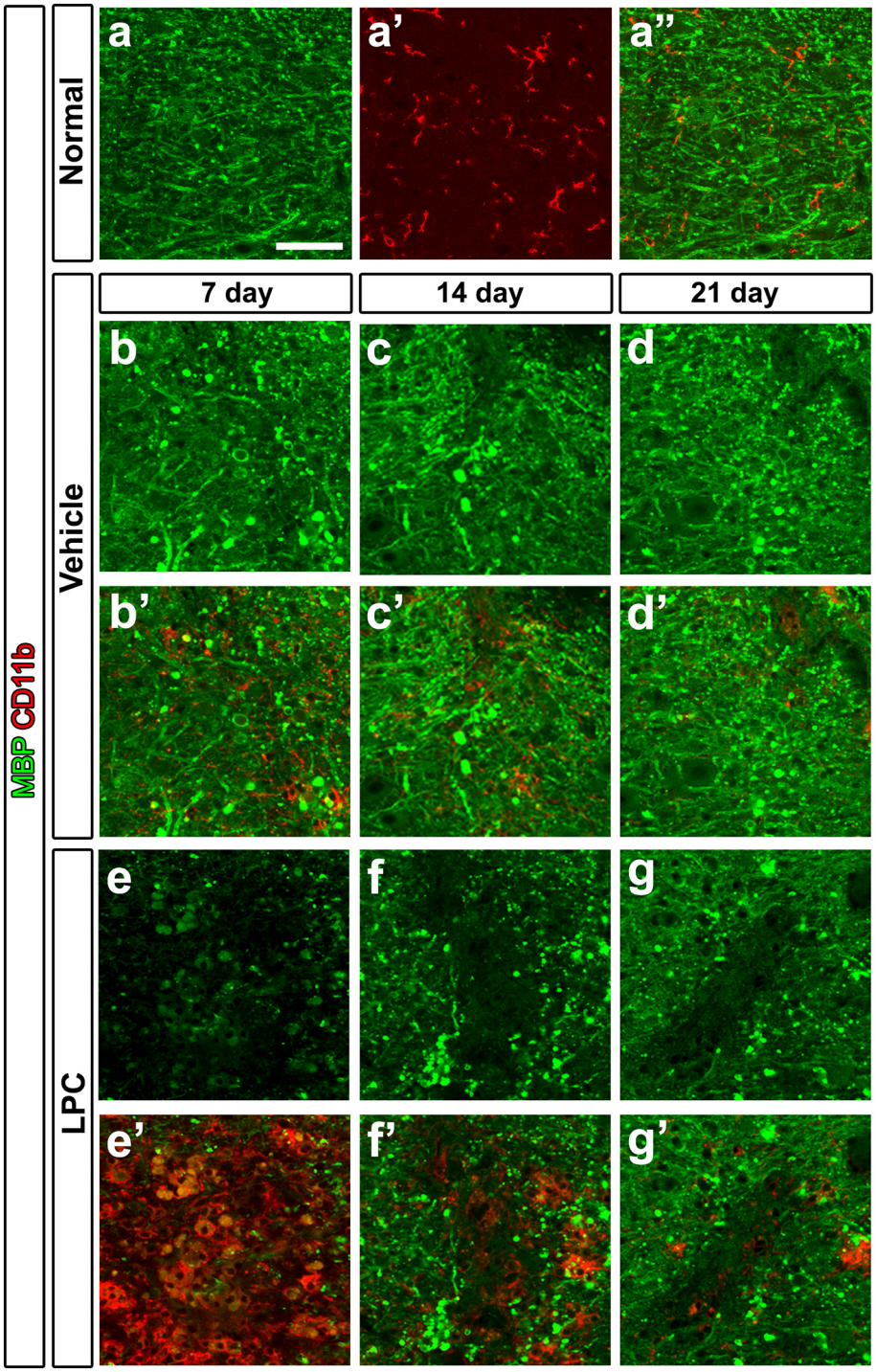

Fig. 1. Confocal images showing time course changes in the loss of the myelin sheath and microglia accumulation at focal lesion area in the 12 N of the medulla oblongata after LPC-injected focal demyelination. Mice received intramedullary injection of 2 μl of 1% LPC or vehicle PBS and then fixed for immunohistochemistry at 7, 14, and 21 days after the injection. Sections were immunostained for a myelin marker MBP and a microglial marker CD11b. (a-a", b, b', c, c', d, d') MBP^+ myelin sheath was disrupted by the insertion of needle and microglia density was slightly increased at 7 days, but they appeared to return to normal after 14 and 21 days. (e, e', f, f', g, g') The intramedullary injection of LPC almost completely eliminated MBP^+ myelin sheath and induced robust microglia accumulation at the lesion area at 7 days. At 14 and 21 days, the density of MBP^+ myelin sheath was likely to increase and alternatively that of microglia decreased. Scale bar = 50 μm.

an early phase of EAE, whereas its proliferation is strongly diminished at a late phase of EAE (Girolamo et al., 2011). Proliferative rate of resident OPCs is largely increase in the spinal cord of EAE-induced mice, but that of NSCs at ependymal layer is not changed (Guo et al., 2011).

Pathological features of MS and EAE include inflammation-induced destruction of the myelin sheath, axonal loss or damage, and activation of microglia and astrocytes (De Stefano et al., 2001; Peterson and Fujinami, 2007). These pathological features have been considered to occur mainly in the forebrain and spinal cord (Compston and Coles, 2008; Martin et al., 1992), whereas several clinical studies indicate that the medulla oblongata is also damaged by MS; it is reported that 50% of MS patients develop medullary atrophy by magnetic resonance imaging (MRI) (Brainin et al., 1987; Nakashima et al., 1999). Moreover, the MRI analysis revealed that decreased volume of the medulla oblongata is relative to the damaged degree of the spinal cord in MS patients (Liptak et al., 2008) Thus, MS is not the only disease of the spinal cord but also that of the whole brain in human (Reich, 2017). On the other hand, the most prominent damages are observed in the spinal cord, while damages are sparse and scattering in the brain of EAE-induced model animals (Schmitt et al., 2012). It is suggested that the disease phenotype and pathological damages in the CNS vary depending on the species and animal strain (Bjelobaba et al., 2018). Most studies about EAE-induced animal model have been reported in the corpus callosum of the forebrain and spinal cord (Chin et al., 2009; Picard-Riera et al.,

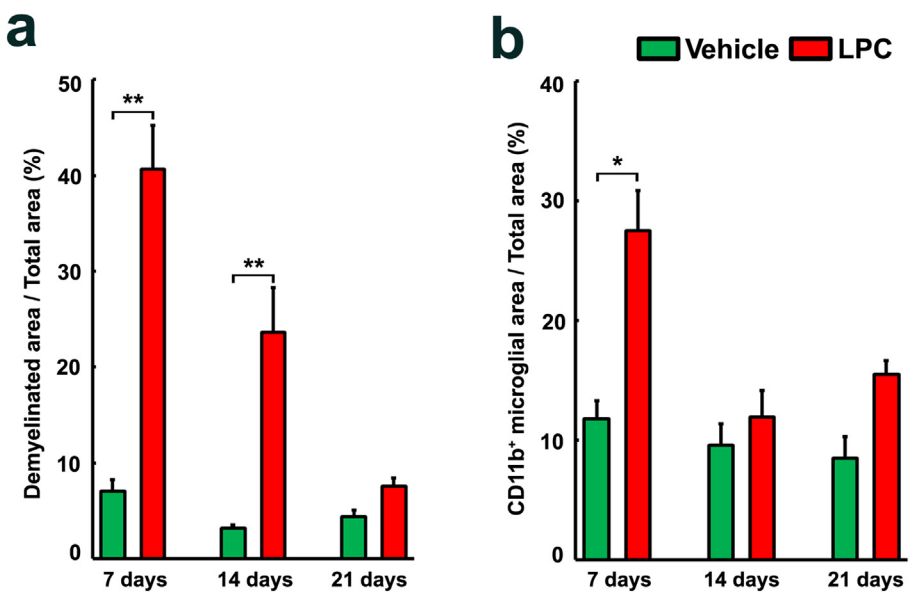

Fig. 2. Quantitative analysis of time course changes in demyelination and microglia accumulation at focal lesion area in the 12 N of the medulla oblongata after LPC injection. Mice received intramedullary injection of 2 µl of 1% LPC or vehicle PBS and then fixed for immunohistochemistry at 7, 14, and 21 days after the injection. (a) The percentage of demyelinated area in the 12 N was significantly increased at 7 and 14 days after LPC injection compared with that of vehicle-treated control. The demyelinated area was calculated by measuring the area that almost completely lacked MBP^+ myelin sheath. (b) The percentage of $CD11b^+$ microglial area was significantly higher at 7 days after the LPC injection compared with that of vehicle-treated control. Data were expressed as the mean (± SE) of 4 animals. * $p < .05$, ** $p < .01$ between vehicle by unpaired Student's *t*-test.

2002). Our previous study indicated that astrocytic gliosis, the proliferation of OPCs, and remyelination occurred in the medulla oblongata of EAE-induced mice (Hiratsuka et al., 2018).

The proliferation of OPCs is largely increased by increased expression of OPC mitogens in response to demyelination (McTigue and Tripathi, 2008). Platelet-growth factor (PDGF) is a most potent mitogen for OPCs and maintains OPCs in a prolonged state of mitosis when combined with fibroblast growth factor-2 (FGF-2) *in vitro* (Bogler et al., 1990). PDGF overexpression in astrocytes significantly increases OPC density within LPC-induced demyelinated area of the spinal cord, but it does not change time course or extent of remyelination (Woodruff et al., 2004). Moreover, the transplantation of PDGF-overexpressing OPCs promotes the proliferation, survival, migration, and maturation of OPCs in injured spinal cord (Yao et al., 2017). VEGF is reported to be highly expressed in acute and chronic MS plaques (Proescholdt et al., 2002) and induces the proliferation and migration of OPCs *in vitro* (Choi et al., 2018; Hayakawa et al., 2011). FGF-2 signaling is required for repopulation of oligodendrocytes in the corpus callosum of mice after cuprizone-induced demyelination (Furusho et al., 2015) and in the spinal cord of EAE-induced animals (Ruffini et al., 2001). Loss-of-function of epidermal growth factor receptor (EGFR) signaling impairs the proliferation of OPCs and remyelination in the corpus callosum after LPC-induced focal demyelination (Aguirre and Gallo, 2007). In contrast, intraventricular infusion of epidermal growth factor (EGF) causes the proliferation of NSCs and OPCs in the SVZ (Doetsch et al., 2002; Gonzalez-Perez et al., 2009) and the overexpression of EGFR in the SVZ and corpus callosum expands OPCs population and promotes oligodendrocyte generation from NSCs in the SVZ and axonal myelination (Aguirre and Gallo, 2007).

The SVZ is far from the medulla oblongata and hence has no potential for a NSC niche to generate new oligodendrocytes, but recently NSC niches have been reported in the area postrema (AP) and central canal (CC) of the medulla oblongata. NSCs in the AP and/or CC are able to supply new oligodendrocytes into the nucleus of the solitary tract (Sol) and hypoglossal nucleus (12 N) under physiologically normal condition (Furube et al., 2015; Miyata, 2015). In EAE-induced mouse, moreover, they are able to supply new oligodendrocytes to replace damaged or lost oligodendrocytes (Hiratsuka et al., 2018). In this study, we examined the dynamics of NSCs and OPCs and VEGF- and PDGF-dependent proliferation of OPCs in the medulla oblongata after LPC-induced focal demyelination. We showed (1) the proliferation of OPCs was dramatically elevated in LPC-induced demyelinated mice, whereas the proliferation and differentiation of NSCs were not changed, (2) both VEGFRs- and PDGFRs-associated tyrosine kinase inhibitors suppressed demyelination-induced proliferation of OPCs. These results indicate that resident OPCs, but not NSCs, are responsible for remyelination of the medulla oblongata during LPC-induced focal demyelination and their proliferation depends on VEGF and PDGF signaling.

2. Methods

2.1. Animals

Adult male wild-type C57BL/6 J mice (8–12 weeks old) were used in this study. In some experiment, we used Nestin-CreERT2/CAG-CATloxP/loxP-EGFP mice. Nestin-CreERT2 mice (Imayoshi et al., 2006; Okada et al., 2006) were crossed to CAG-CATloxP/loxP-EGFP mice (Kawamoto et al., 2000) to obtain Nestin-CreERT2/CAG-CATloxP/loxP-EGFP mice. All mice were housed under specific pathogen-free conditions, dark/light cycle of 12 h, room temperature at 23–25 °C, and free access to food and water. All experiments were performed according to the Guidelines laid down by the Proper Conduct of Animal Experiments Science Council of Japan. The experimental protocol was approved by the Animal Ethics Experimental Committee of the Kyoto Institute of Technology.

2.2. Treatment of animals

LPC-induced demyelination. For the LPC injection, a 33G needle attached to a microsyringe (Hamilton Company, Reno, NV) was implanted in each mouse under anesthesia with isoflurane so that its tip laid in the 12 N at 7.5-mm posterior and 0.25-mm lateral to bregma at a depth of 3.5 mm from the skull surface using a standard stereotaxic technique (Paxinos and Franklin, 2007). Mice then received 2 µl of 1% LPC (Sigma-Aldrich, Millipore Sigma, Burlington, MA; 3 µl, 0.5 µl/min) in phosphate-buffered saline (PBS; pH 7.4) using a Model EP-1000E administration pump (Melquest, Toyama, Japan). As a vehicle control, the same volume of the PBS was injected into the 12 N. Animals were sacrificed for immunohistochemistry after 7, 14, 21, and 28 days after the LPC injection.

Injection of tyrosine kinase inhibitors for VEGFRs and PDGFRs. VEGFR-associated tyrosine kinase inhibitor AZD2171 (Hanrahan and Heymach, 2007) and PDGFR-associated tyrosine kinase inhibitor STI-571 (Wedge et al., 2005) were purchased from LKT Laboratories Inc. (St Paul, MN). Mice received the oral administration of 0.2 ml of AZD2171 (6 mg/kg/day) in 1% Tween-80 and STI-571 (200 mg/kg/day) in distilled

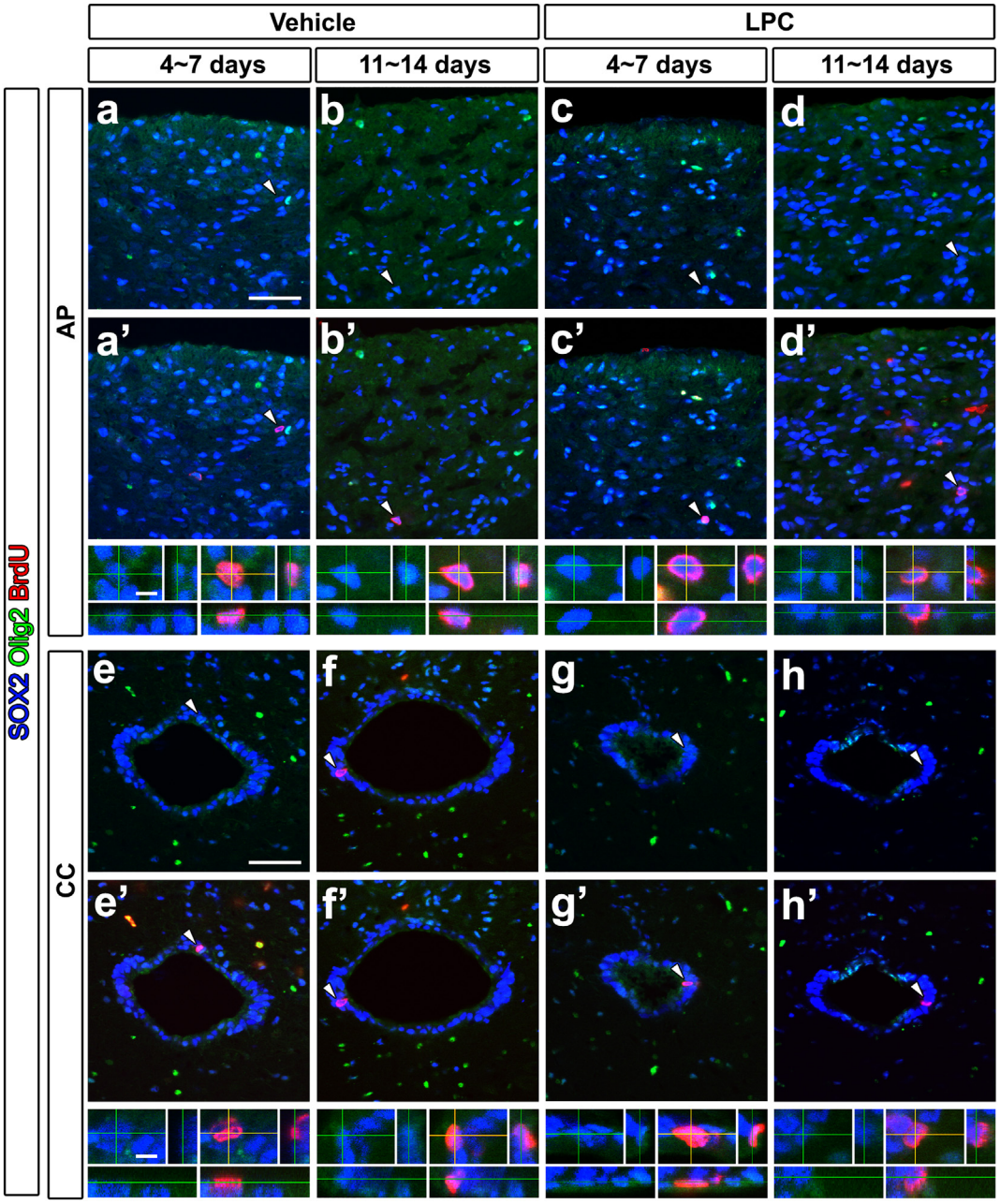

Fig. 3. Proliferation of NSCs in the AP and CC of the adult mouse after LPC-injected focal demyelination. Mice received 3-day access to the water containing BrdU (1 mg/ml) during 4–7 and 11–14 days after the injection of LPC or vehicle and then fixed to detect proliferating cells by BrdU immunohistochemistry. $Sox2^+$ and $Olig2^-$ cells were estimated as NSCs. (a-d, a'-d') The number of BrdU-labeled $Sox2^+$ and $Olig2^-$ astrocyte-like NSCs (arrowheads) in the AP was not different between vehicle- and LPC-injected mice. (e-h, e'-h') The injection of LPC did not change the number of BrdU-labeled $Sox2^+$ and $Olig2^-$ tanycyte-like NSCs (arrowheads) in the CC. Three-dimensional analysis revealed the presence of BrdU-labeled nuclei in $Sox2^+$ NSCs (bottom panels in a'-d' and e'-h'). Scale bars = 50 (a, e) and 10 (bottom panels in a', e') μm.

deionized water twice daily for 3 days.

2.3. Assay for cell proliferation and differentiation

For detecting proliferating cell, we used the immunohistochemistry of a thymidine analog bromodeoxyuridine (BrdU; Sigma-Aldrich) after drinking of BrdU-containing water (1 mg/ml) for 3 days. Nestin-CreERT2/CAG-CATloxP/loxP-EGFP mice received consecutive 3-day intraperitoneal injection tamoxifen (Toronto Research Chemicals Inc., Ontario Canada) at 60 mg/kg before the LPC injection and fixed 28 days after the LPC injection.

2.4. Tissue preparation and immunohistochemistry

For light microscopy, mice were perfused with PBS (pH 7.4) containing 0.1% trisodium citrate dihydrate followed by 4% paraformaldehyde (PFA) in 0.1 M phosphate buffer (PB; pH 7.4) under anesthesia with isoflurane. The brains were carefully dissected out and post-fixed overnight at 4 °C in the same fixative. Fixed tissue was immersed in PBS containing 30% sucrose and then frozen quickly in Tissue-Tek OCT compound (Sakura Finetechnical, Tokyo, Japan). The fixed brains were cut coronally at a thickness of 30 μm by a cryostat (Leica, Wetzlar, Germany) Sections were washed with PBS and treated with 25 mM glycine in PBS for 20 min to quench the remaining fixative

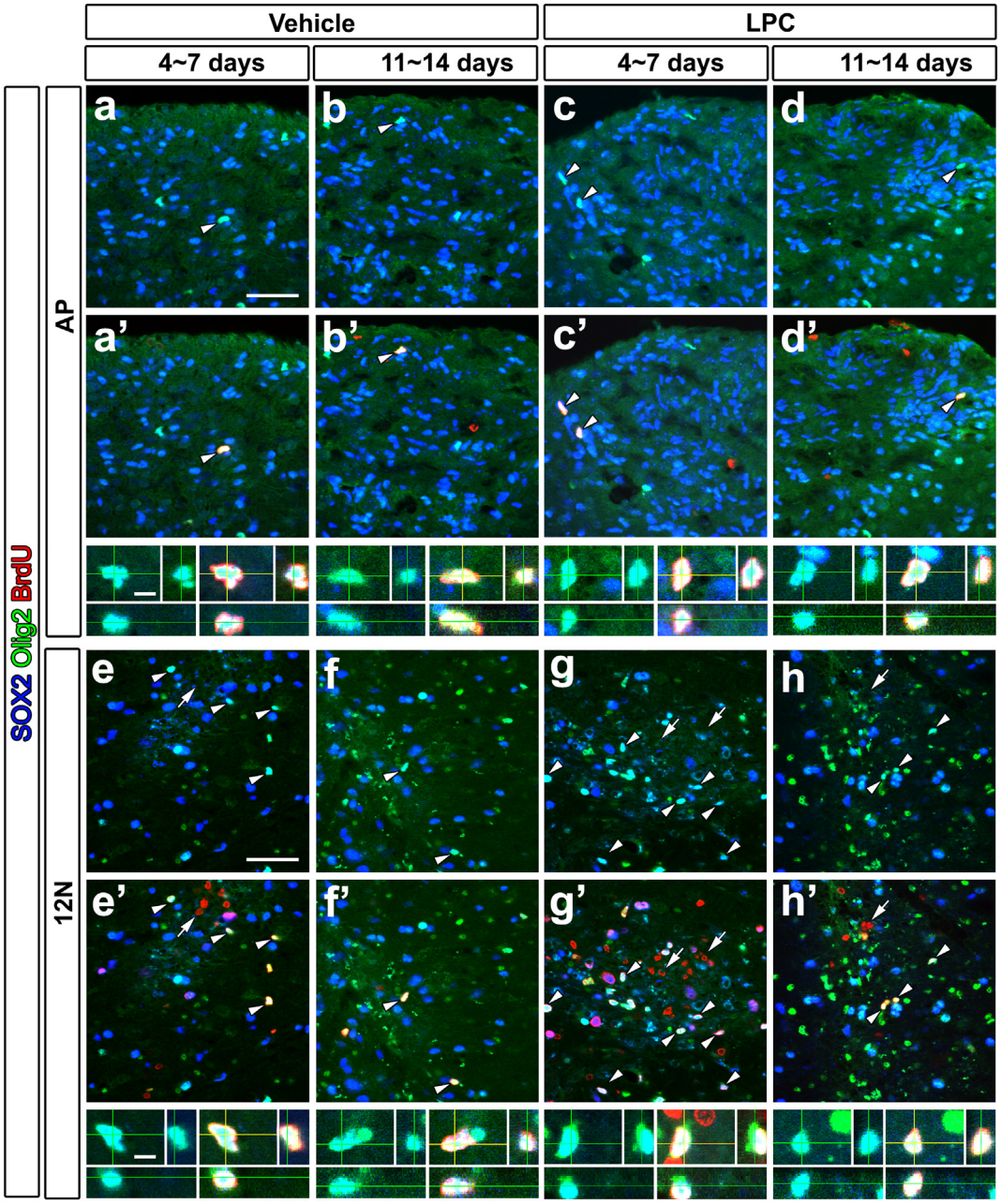

Fig. 4. Proliferation of OPCs in the AP and 12 N of the adult mouse after LPC-injected focal demyelination. Mice received 3-day access to the water containing BrdU (1 mg/ml) during 4–7 and 11–14 days after the injection of LPC or vehicle and then fixed to detect proliferating cells by BrdU immunohistochemistry. $Sox2^+$ and $Olig2^+$ cells were identified as OPCs. (a-d, a'-d') In the AP, BrdU-labeled $Sox2^+$ and $Olig2^+$ OPCs (arrowheads) were sometimes seen in both LPC- and vehicle-injected animals. (e-h, e'-h') In the 12 N, BrdU-labeled $Sox2^+$ and $Olig2^+$ OPCs (arrowheads) were observed more frequently in LPC-injected mice than vehicle-injected ones. BrdU-labeled $Sox2^-$ and $Olig2^-$ cells (arrows), presumably microglia, were seen more often in LPC-injected mice compared with vehicle-injected animals. Three-dimensional analysis revealed the presence of BrdU-labeled nuclei in $Sox2^+$ and $Olig2^+$ OPCs (bottom panels in a'-d' and e'-h'). Scale bars = 50 (a, e) and 10 (bottom panels in a', e') μm.

aldehyde and then incubated with 5% normal goat serum (NGS) in PBS containing 0.3% Triton X-100 (PBST) at 4 °C for 24 h. They were incubated with the primary antibody at 4 °C for 48–72 h and then treated with Alexa405-, Alexa488-, or Alexa594-conjugated secondary antibody (Jackson ImmunoResearch, West Grove, PA, USA; dilution 1:400) in PBST for 2 h. When mouse primary antibody was used, sections were treated with goat Fab fragment against mouse IgG (Jackson ImmunoResearch; dilution 1:400) for 2 h before using primary antibody and Alexa488-conjugated goat F(ab)2 fragment against mouse IgG was used (Jackson ImmunoResearch; dilution 1:100) to prevent from non-specific binding of endogenous mouse Fc receptors. Primary antibodies used in this study were adenomatous polyposis coli (APC; mouse IgG; clone CC1, Millipore-Chemicon, Billerica, MA; dilution 1:800), BrdU (rat IgG; Clone BU1/75, Abcam, Cambridge, United Kingdom; dilution 1:1000), CD11b (rat IgG, clone 5C6, BIO-RAD; dilution; 1:10,000), glial fibrillary acidic protein (GFAP; guinea pig IgG; YN-GFAP2012-Pig; dilution 1:400, Nakano et al., 2015), GFP (rabbit IgG; Molecular Probes, ThermoFisher, Eugene, OR; dilution 1:1000), myelin basic protein (MBP; rabbit IgG; DAKO, Glostrup, Denmark; dilution; 1:1000), oligodendrocyte transcription factor 2 (Olig2; rabbit IgG; Millipore-Chemicon; dilution 1:500), sex determining region Y-box 2 (SOX2; goat IgG; Millipore-Chemicon; dilution 1:2000). The experimental procedure

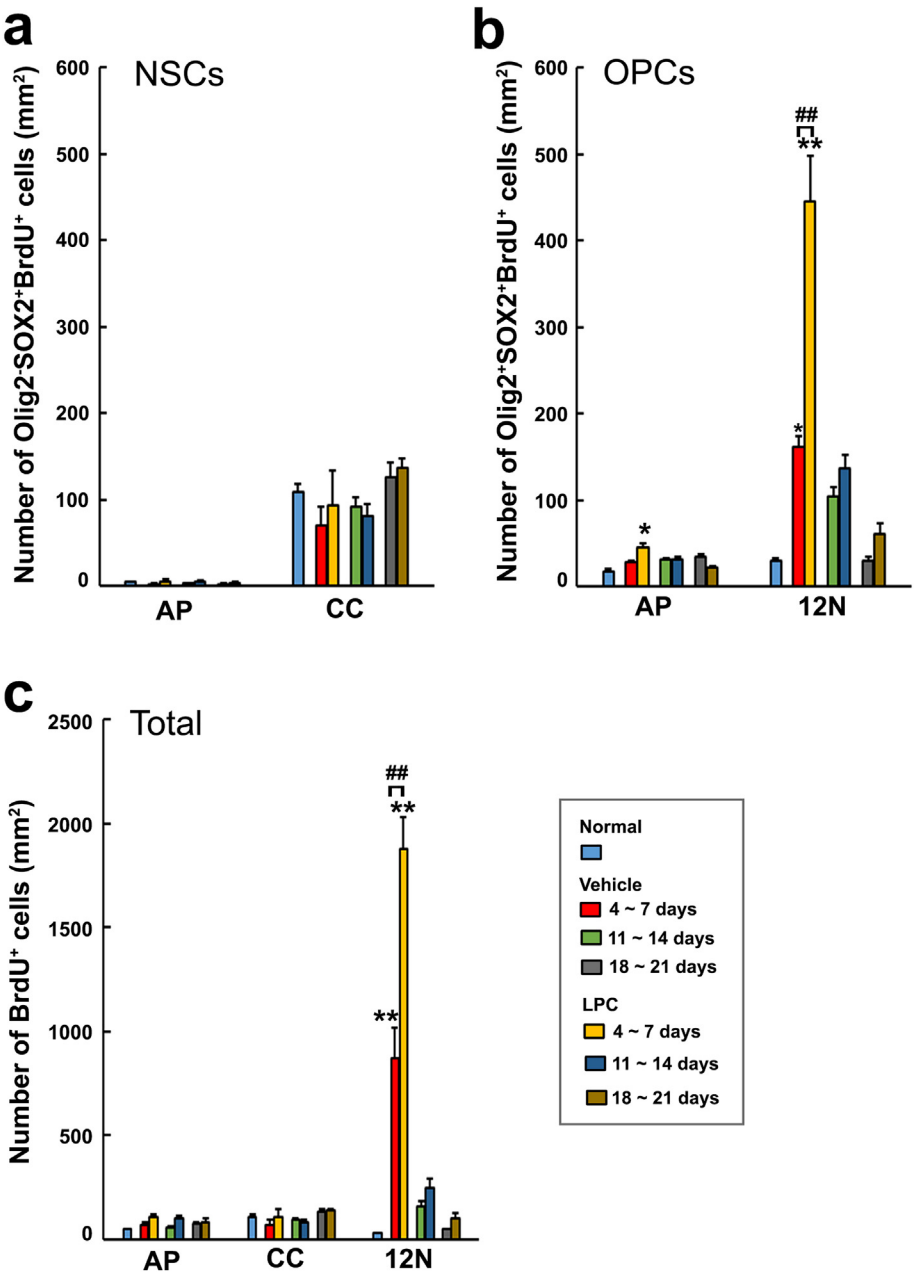

Fig. 5. Quantitative analysis of the number of BrdU-labeled NSCs and OPCs in the medulla oblongata after LPC-injected focal demyelination. Mice received 3-day access to the water containing BrdU (1 mg/ml) during 4–7, 11–14, and 18–21 days after the injection of LPC or vehicle and then fixed to detect proliferating cells by BrdU immunohistochemistry. (a) The number of BrdU-labeled $Sox2^+$ and $Olig2^-$ NSCs in the AP and CC was not significantly among LPC- and vehicle-injected mice and normal control. (b) The number of BrdU-labeled $Sox2^+$ and $Olig2^+$ OPCs in the AP and 12 N significantly higher in LPC- injected mice than that of vehicle-injected animals at the early period of remyelination. The injection of vehicle PBS also significantly increased the number of BrdU-labeled $Sox2^+$ and $Olig2^+$ OPCs in the 12 possibly because of mechanical destruction by the insertion of a needle. (c) The total number of BrdU-labeled cells in the 12 N was significantly increased LPC- injected mice than that of vehicle-injected ones at the early period of remyelination. Data were expressed as the mean (± SE) of 4 animals. * $p < .05$, ** $p < .01$ between normal and vehicle or normal and LPC and ## $p < .01$ between vehicle and LPC by ANOVA with Tukey posy hoc test.

of BrdU immunohistochemistry was performed according to our previous studies (Furube et al., 2014; Hiratsuka et al., 2018). Briefly, the sections were incubated with 2 N HCl at 37 °C for 30 min and neutralized with 0.1 M PB (pH 8.4), and 5% NGS in PBST for 24 h. For visualization of BrdU, the sections were incubated with rat anti-BrdU IgG in PBST containing 1% NGS for 48–72 h at 4 °C and then with Alexa594-conjugated anti-rat IgG antibody in PBST for 2 h.

2.5. Confocal analysis & statistical analysis

The coverslips were sealed with Vectashield (VectorLabs, Burlingame, CA) and laser-scanning confocal microscopes (Fluoview, FV10i, OLYMPUS, Tokyo, Japan and LSM 510, CarlZeiss, Oberkochen, Germany) were used for the observation. Confocal images (1024 × 1024 pixels) were saved as TIF files by employing Olympus FV10-ASW ver 1.7 viewer or LSM510 META Image Browser 4.2.0.121 for Windows. In quantification data, the number of BrdU-labeled proliferating cells and EGFP-positive cells were counted by using Winroof. The threshold intensity of which was set to include measurement profiles by visual inspections and was kept constant. An analysis of all images was performed such that the experimenter was blind to the treatment group. At least 10 sections per animal were selected from the AP, CC, and 12 N of the medulla oblongata according to the mouse brain atlas (Paxinos and Franklin, 2001) and the density of BrdU-labeled or EGFP-positive cells in each animal was obtained by calculating total number of BrdU-labeled or EGFP-positive cells / total area examined. Statistical difference was assessed using a significance level of $p < .05$ with unpaired Student's *t*-test and ANOVA with Tukey *post hoc* test.

3. Results

3.1. Remyelination in the 12 N after LPC-induced demyelination

Mice received intramedullary injection of 2 µl of 1% LPC or vehicle into the 12 N of the medulla oblongata of adult mice. Confocal images

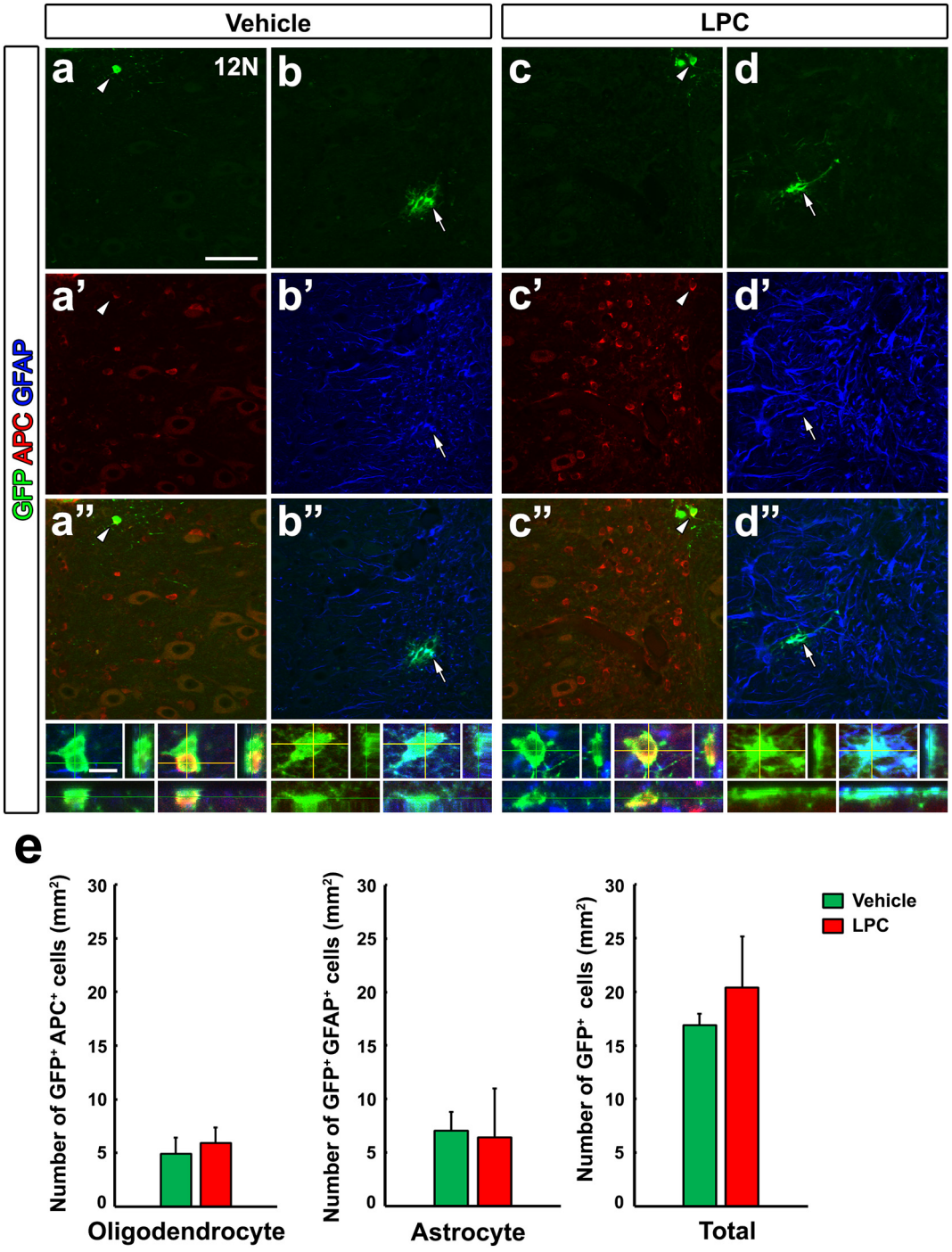

Fig. 6. Fate determination of NSCs by Nestin-CreERT2/CAG-CATloxP/loxP-EGFP transgenic adult mice after LPC-injected focal demyelination. The Nestin-CreERT2/CAG-CATloxP/loxP-EGFP transgenic mice received consecutive 3-day intraperitoneal injection of 0.2 mg/kg tamoxifen 7 days before the LPC injection and sacrificed at 28 days after the LPC injection. (a-a", b-b", c-c", d-d") EGFP-expressing APC$^+$ oligodendrocytes (arrowheads) and GFAP$^+$ astrocytes (arrows) were rarely seen in the 12 N of vehicle- and LPC-injected mice. Three-dimensional analysis revealed the presence of EGFP in APC$^+$ oligodendrocyte and GFAP$^+$ astrocyte (bottom panels in a"-d"). Scale bars = 50 (a) and 10 (bottom in a') μm. (e) The quantitative analysis revealed that the number of EGFP-expressing APC$^+$ oligodendrocytes and GFAP$^+$ astrocytes was not significantly different between vehicle- and LPC-injected animals. The total number of EGFP-expressing cells was also not significantly different between vehicle- and LPC-injected animals. Data were expressed as the mean (± SE) of 4 animals. Statistical analysis was done by Student's t-test.

showed that the density of MBP-positive myelin sheath was not different between normal and vehicle-injected mice, although a slight mechanical damage by injected needle appeared to occur in vehicle-injected ones (Fig. 1a-a", b-d, b'-d'). The density of MBP-positive myelin sheath was apparently lower in LPC-injected mice (Fig. 1e, e') compared with that of vehicle-injected control (Fig. 1b, b') at 7 days after the injection. The density of MBP-positive myelin sheath was increased at 14 and 21 days after the injection (Fig. 1f, f', g, g'). On the other hand, the density of CD11b-positive microglia was higher in LPC-injected mice (Fig. 1e') compared with that of vehicle-injected animals (Fig. 1b') at 7 days after the injection and then it was decreased along with the progress of remyelination (1f', g').

The quantitative analysis revealed that demyelinated area in the 12 N was significantly higher at 7 and 14 days after the injection and

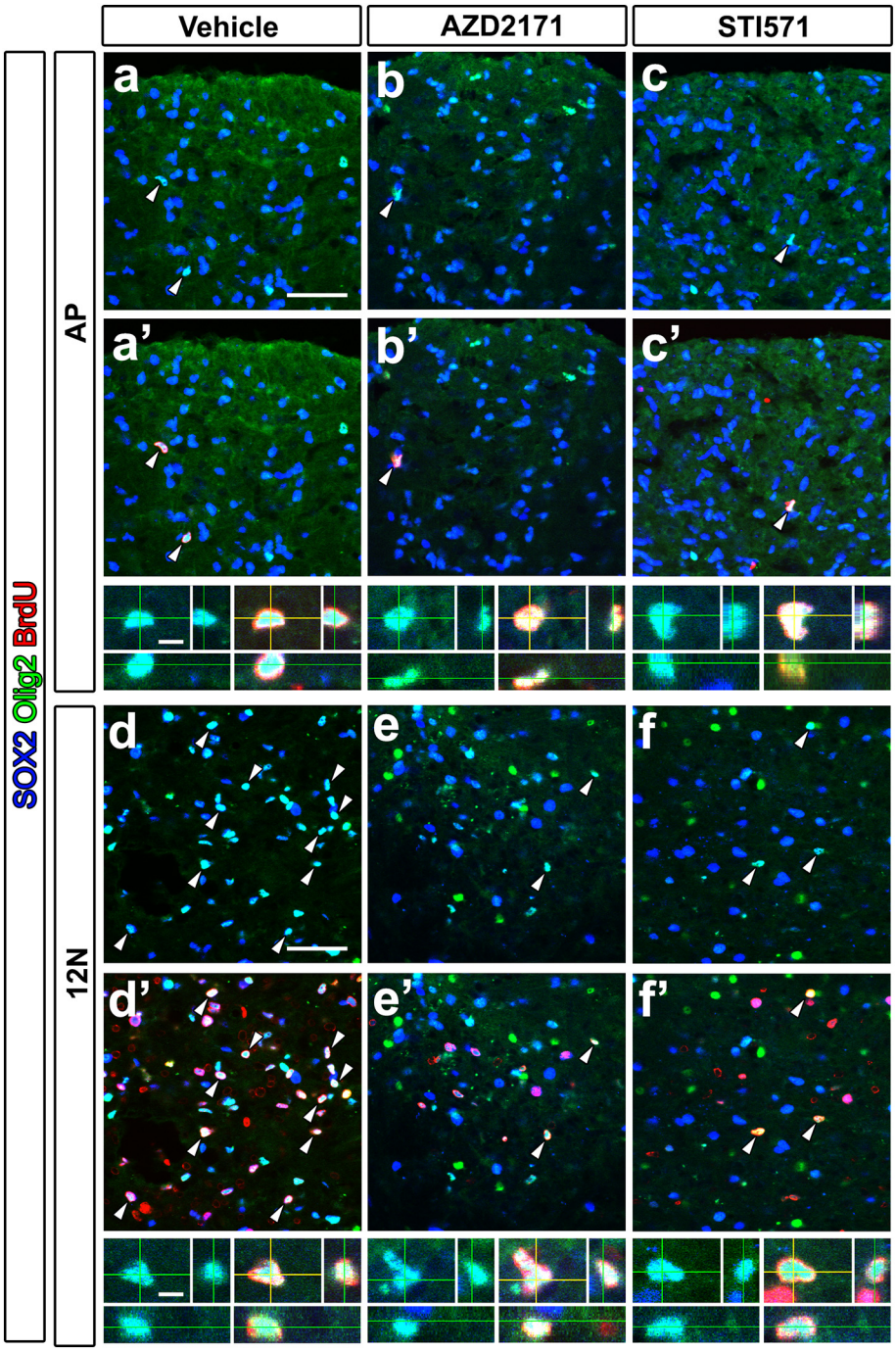

Fig. 7. Effects of tyrosine kinase inhibitors for VEGFRs or PDGFRs on LPC-induced proliferation of OPCs in the AP and 12 N of adult mice. Mice received 3-day consecutive oral administration of the tyrosine kinase inhibitor AZD2171 for VEGFRs (6 mg/kg per day) and STI571 for PDGFRs (200 mg/kg per day) together with the drinking of BrdU-containing water (1 mg/ml) at 4–7 days after the LPC injection. (a-c, a'-c') BrdU-labeled Sox2$^+$ and Olig2$^+$ OPCs were sometimes seen in the AP of vehicle- and inhibitor-treated mice. (d-f, d'-f') There were many BrdU-labeled Sox2$^+$ and Olig2$^+$ OPCs in the 12 N of LPC- and vehicle-treated mice, whereas oral administration of AZD2171 and STI571 largely diminished the number of BrdU-labeled Sox2$^+$ and Olig2$^+$ OPCs. Three-dimensional analysis revealed the presence of BrdU nuclei in Sox2$^+$ and Olig2$^+$ OPCs (bottom panels in a'-c' and d'-f'). Scale bars = 50 (a, d) and 5 (bottom panels in a', d') μm.

returned to vehicle control level at 21 days compared with the vehicle (Fig. 2a). In contrast, the area of CD11b$^+$ microglia was significantly higher at 7 days after the injection and returned to vehicle control level at 14 and 21 days compared with the vehicle (Fig. 2b).

3.2. Proliferation of NSCs and OPCs after LPC-induced demyelination

To examine cellular proliferation, mice received drinking of BrdU-containing water for 3 days at various days after the LPC injection. The proliferation of SOX2$^+$ and Olig2$^-$ NSCs was not changed in the AP of LPC-injected mice at 7 and 14 day (Fig. 3c, c', d, d') compared with the vehicle control (Fig. 3a, a', b, b') and normal animals (Supplementary Fig. 1a, a'). Similarly, the proliferation of SOX2$^+$ and Olig2$^-$ NSCs in the CC was not changed in LPC-injected mice (Fig. 3e, e', f, f') compared with vehicle-injected animals (Fig. 3g, g', h, h') or normal ones (Supplementary Fig. 1b, b').

On the other hands, the proliferation of SOX2$^+$ and Olig2$^+$ OPCs was increased in the AP and 12 N of LPC-injected mice (Fig. 4c,c', g, g') compared with vehicle-injected animals (Fig. 4a, a', e, e') at 7 days after injection. The proliferation of SOX2$^+$ and Olig2$^+$ OPCs in the 12 N of vehicle-injected mice was higher than normal condition, whereas that of the AP was not changed (Supplementary Fig. 2). The proliferation of SOX2$^+$ and Olig2$^+$ OPCs returned to control levels at 14 days after LPC injection (Fig. 4b, b', d, d', f, f', h, h'). The quantitative analysis revealed that the number of BrdU-labeled SOX2$^+$ and Olig2$^-$ NSCs was not changed in the AP and CC of LPC-injected mice at 7, 14, and 21 days (Fig. 5a). The density of BrdU-labeled cells in each animal was obtained the total number of BrdU-labeled cells / total area examined. Astrocyte-

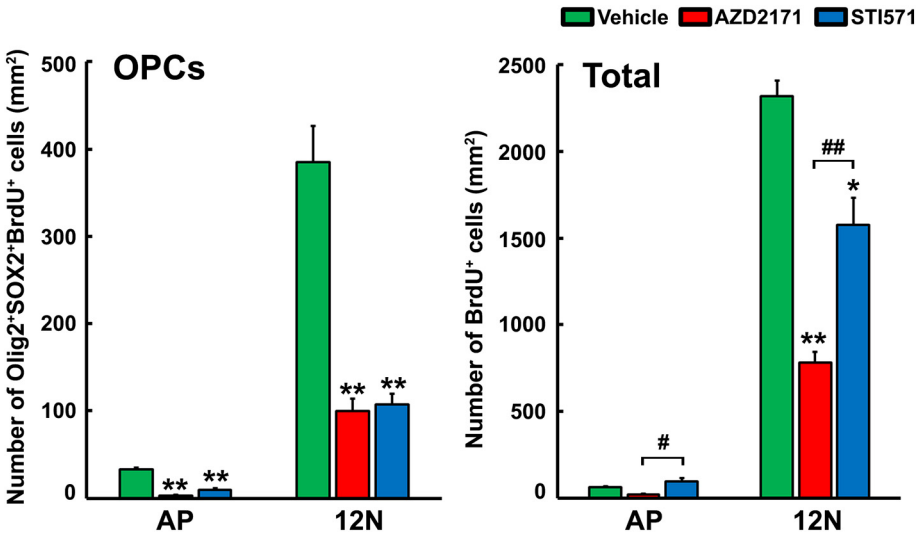

Fig. 8. Quantitative analysis of effects of tyrosine kinase inhibitors for VEGFRs or PDGFRs on LPC-induced proliferation of OPCs in the AP and 12 N of adult mice. Mice received 3-day consecutive oral administration of the tyrosine kinase inhibitor AZD2171 for VEGFRs (6 mg/kg per day) and STI571 for PDGFRs (200 mg/kg per day) together with the drinking of BrdU-containing water (1 mg/ml) at 4–7 days after LPC injection. The number of BrdU-labeled OPCs in the AP and 12 N was significantly decreased by the treatment with AZD2171 and STI571 compared with that of vehicle-treated control. The total number of BrdU-labeled cells was significantly decreased in the 12 N by the treatment with AZD2171 and STI571 compared with that of the vehicle control. Data were expressed as the mean (± SE) of 4 animals. * $p < .05$, ** $p < .01$ between vehicle and AZD2171 or STI571 and # $p < .05$, ## $p < .01$ between AZD2171 and STI571 by ANOVA with Tukey posy hoc test.

like NSCs scatteringly distributed throughout a broad area of the AP and therefore the density was relatively low, but tanycyte-like NSCs localized in a narrow area of ependymal regions facing to the CC and thus the density was relatively high. On the other hand, the number of BrdU-labeled SOX2$^+$ and Olig2$^+$ OPCs elevated in the 12 N of LPC-treated mice at 7 days, but it was not altered at 14 and 21 days (Fig. 5b). The total number of BrdU-labeled cells increased in the 12 N at 7 and 14 days, whereas it was not changed in the AP and CC (Fig. 5c).

3.3. Fate of NSCs after LPC-induced demyelination

To examine the generation of new oligodendrocyte from NSCs in the medulla oblongata after LPC-induced demyelination, Nestin-CreERT2/CAG-CATloxP/loxP-EGFP mice were used. NSCs and their progeny were detected by the expression of EGFP after the treatment of tamoxifen. There were a few GFP$^+$ and APC$^+$ oligodendrocytes (Fig. 6a-a") and GFP$^+$ and GFAP$^+$ astrocytes (Fig. 6b-b") in the 12 N of vehicle-injected mice. The number of GFP$^+$ and APC$^+$ oligodendrocytes was not changed by LPC-injected mice compared with that of the vehicle-injected ones (Fig. 6c-c"). Similarly, the number of GFP$^+$ and GFAP$^+$ astrocytes was not changed in LPC-injected mice compared with that of the vehicle-injected ones (Fig. 6d-d"). The quantitative analysis revealed the number of GFP$^+$ and APC$^+$ oligodendrocytes and GFP$^+$ and GFAP$^+$ astrocytes was not changed between LPC- and vehicle-injected animals (Fig. 6e). The total number of GFP$^+$ cells was also not changed in LPC-injected mice compared with that of vehicle-injected animals.

3.4. Effect of VEGF and PDGF signaling inhibition on OPC proliferation after LPC-induced demyelination

To examine whether the proliferation of OPCs is regulated by VEGF and/or PDGF signaling, we used selective VEGFR- and PDGF-associated tyrosine kinase inhibitor AZD2171 and STI571, respectively. Mice received 3-day oral injection of AZD2171 (6 mg/kg per day) or STI571 (200 mg/kg per day) together with drinking of BrdU from day 4–7 after the LPC injection. The treatment of AZD2171 and STI571 appeared to decrease the number of BrdU-labeled SOX2$^+$ and Olig2$^+$ OPCs in the AP (Fig. 7b, b', c, c') compared with that of vehicle-treated ones (Fig. 7a, a'). The treatment of AZD2171 and STI571 apparently decreased the number of BrdU-labeled SOX2$^+$ and Olig2$^+$ OPCs in the 12 N (Fig. 7e, e', f, f') compared with that of vehicle-treated ones (Fig. 7d, d').

The quantitative analysis showed that the treatment of AZD2171 and STI571 remarkably decreased the number of BrdU-labeled SOX2$^+$ and Olig2$^+$ OPCs in the AP and 12 N compared with that of vehicle-treated mice (Fig. 8). The total number of BrdU-labeled cells was prominently decreased in the 12 N by the treatment of AZD2171 and STI571 compared with that of vehicle-treatment, whereas such decrease was not observed in the AP.

4. Discussion

Until now, few pieces of researches have been reported for remyelination in the medulla oblongata, because most studies for remyelination in the CNS have been focused on the spinal cord and forebrain. The main findings of our present study are as follows; 1) Resident OPCs are responsible for remyelination to repair damaged area in the medulla oblongata after LPC-induced focal demyelination, whereas NSCs do not contribute to this repair process. 2) VEGFRs- and PDGFRs-signaling is crucial for the proliferation of OPCs in the medulla oblongata after LPC-induced demyelination.

In the present study, the proliferation of resident OPCs was largely enhanced in the 12 N after LPC-induced focal demyelination. This result well coincides with our previous study in EAE-induced demyelination that OPCs generate mature oligodendrocyte in the 12 N, paramedian reticular nucleus, and ventral part of medullary reticular nucleus of the medulla oblongata (Hiratsuka et al., 2018). It is also reported in the forebrain and spinal cord that LPC-induced focal demyelination largely promote the proliferation of OPCs (Gensert and Goldman, 1997; Kataria et al., 2018; Nait-Oumesmar et al., 1999). Thus, it is possible that the proliferation and differentiation of resident OPCs have a major contribution in remyelination in the medulla oblongata as the forebrain and spinal cord during focal remyelination.

Our present study showed that NSC-derived OPCs were not changed for remyelination of the medulla oblongata after LPC-induced focal demyelination. A similar result is reported in remyelination of the spinal cord during EAE-induced demyelination (Guo et al., 2011). In contrast, the present result differs from reports of other brain regions that NSCs in the SVZ can supply oligodendrocytes into the corpus callosum and striatum after LPC-induced focal demyelination (Capilla-Gonzalez et al., 2013; Menn et al., 2006). The present result is also different from our previous study that the number of NSC-derived mature oligodendrocyte was increased in EAE-induced mice (Hiratsuka et al., 2018). These differences are probably because NSCs have unique characteristics depending on each CNS region and medullary NSCs have different properties compared with NSCs in the SVZ. Resident OPCs only perform sufficient supply without NSCs in the medulla oblongata, because LPC-induced demyelination damage is smaller area and shorter period compared with EAE-induced one. Taken together with the previous studies, this study indicates that resident OPCs are more

preferential contribution to repair the myelin sheath compared with NSCs and NSCs contribute in the case of severe demyelinated damage in the medulla oblongata.

Many studies have shown that various growth factors are important in oligodendrocyte proliferation and remyelination in the rodent forebrain and spinal cord (McTigue and Tripathi, 2008). On the other hand, the importance of VEGF signaling has not been proven in the CNS *in vivo*. The treatment of AZD2171 decreased proliferation of OPCs in the 12 N of the medulla oblongata after LPC-induced focal demyelination. VEGF signaling is required for the proliferation of OPCs of the medulla oblongata after LPC-induced focal demyelination. VEGF is reported to be highly expressed in acute and chronic MS plaques (Proescholdt et al., 2002) and induces proliferation and migration of OPCs *in vitro* (Choi et al., 2018; Hayakawa et al., 2011). Recently, it is reported that OPCs migrate along the abluminal endothelial surface of nearby blood vessels and OPC migration is disrupted with defective vascular architecture in developing brains (Tsai et al., 2016). Migration of OPCs into demyelinated areas is considered to be critical in human diseases such as multiple sclerosis and hypoxic injury (Franklin and Ffrench-Constant, 2008). Thus, our present study provides the first direct evidence that VEGF signaling is critical in the proliferation and/or migration of OPCs in adult brains.

In our present study, it is also shown that the treatment of STI571 decreased the proliferation of OPCs in the 12 N of medulla oblongata after LPC-induced focal demyelination. It is reported that expression of PDGF is up-regulated in MS patients (Harirchian et al., 2012; Mori et al., 2014; Mori et al., 2013). PDGF signaling induced repopulation of OPCs and remyelination in the corpus callosum and spinal cord of rodents (Woodruff et al., 2004; Yao et al., 2017). Thus, our present result well coincides with the previous studies about the proliferation of OPCs in the corpus callosum and spinal cord. Thus, the present study suggests that the activation of VEGF and PDGF signaling can be a strategy of remyelination in the medulla oblongata.

Acknowledgements

This work was supported in part by Scientific Research Grants from The Japan Society for the Promotion of Science (No. 16K07027, K1906921) and Research Fellowship of the Japan Society for the Promotion of Science for Young Scientists (No. 16J10225). We are grateful to Drs. H. Okano, R. Kageyama, J. Miyazaki, and Francois Renault-Mihara for generous supplies of Nestin-CreERT2 and CAG-CATloxP/loxP-EGFP transgenic mice, respectively.

Appendix A. Supplementary data

Supplementary data to this article can be found online at https://doi.org/10.1016/j.jneuroim.2019.04.016.

References

Aguirre, A., Gallo, V., 2007. Reduced EGFR signaling in progenitor cells of the adult subventricular zone attenuates oligodendrogenesis after demyelination. Neuron Glia Biol. 3, 209–220.
Bjelobaba, I., Begovic-Kupresanin, V., Pekovic, S., Lavrnja, I., 2018. Animal models of multiple sclerosis: focus on experimental autoimmune encephalomyelitis. J. Neurosci. Res. 96, 1021–1042.
Bogler, O., Wren, D., Barnett, S.C., Land, H., Noble, M., 1990. Cooperation between two growth factors promotes extended self-renewal and inhibits differentiation of oligodendrocyte-type-2 astrocyte (O-2A) progenitor cells. Proc. Natl. Acad. Sci. U. S. A. 87, 6368–6372.
Brainin, M., Reisner, T., Neuhold, A., Omasits, M., Wicke, L., 1987. Topological characteristics of brainstem lesions in clinically definite and clinically probable cases of multiple sclerosis: an MRI-study. Neuroradiology. 29, 530–534.
Capilla-Gonzalez, V., Cebrian-Silla, A., Guerrero-Cazares, H., Garcia-Verdugo, J.M., Quinones-Hinojosa, A., 2013. The generation of oligodendroglial cells is preserved in the rostral migratory stream during aging. Front. Cell. Neurosci. 7, 147.
Chin, C.L., Pai, M., Bousquet, P.F., Schwartz, A.J., O'Connor, E.M., Nelson, C.M., et al., 2009. Distinct spatiotemporal pattern of CNS lesions revealed by USPIO-enhanced MRI in MOG-induced EAE rats implicates the involvement of spino-olivocerebellar pathways. J. Neuroimmunol. 211, 49–55.
Choi, E.H., Xu, Y., Medynets, M., Monaco, M.C.G., Major, E.O., Nath, A., et al., 2018. Activated T cells induce proliferation of oligodendrocyte progenitor cells via release of vascular endothelial cell growth factor-A. Glia. 66, 2503–2513.
Compston, A., Coles, A., 2008. Multiple sclerosis. Lancet. 372, 1502–1517.
De Stefano, N., Narayanan, S., Francis, G.S., Arnaoutelis, R., Tartaglia, M.C., Antel, J.P., et al., 2001. Evidence of axonal damage in the early stages of multiple sclerosis and its relevance to disability. Arch. Neurol. 58, 65–70.
Dimou, L., Simon, C., Kirchhoff, F., Takebayashi, H., Gotz, M., 2008. Progeny of Olig2-expressing progenitors in the gray and white matter of the adult mouse cerebral cortex. J. Neurosci. 28, 10434–10442.
Doetsch, F., Petreanu, L., Caille, I., Garcia-Verdugo, J.M., Alvarez-Buylla, A., 2002. EGF converts transit-amplifying neurogenic precursors in the adult brain into multipotent stem cells. Neuron. 36, 1021–1034.
Dubois-Dalcq, M., Ffrench-Constant, C., Franklin, R.J., 2005. Enhancing central nervous system remyelination in multiple sclerosis. Neuron. 48, 9–12.
Dupree, J.L., Mason, J.L., Marcus, J.R., Stull, M., Levinson, R., Matsushima, G.K., et al., 2004. Oligodendrocytes assist in the maintenance of sodium channel clusters independent of the myelin sheath. Neuron Glia Biol. 1, 179–192.
Edgar, J.M., Nave, K.A., 2009. The role of CNS glia in preserving axon function. Curr. Opin. Neurobiol. 19, 498–504.
Ffrench-Constant, C., Raff, M.C., 1986. Proliferating bipotential glial progenitor cells in adult rat optic nerve. Nature. 319, 499–502.
Franklin, R.J., Ffrench-Constant, C., 2008. Remyelination in the CNS: from biology to therapy. Nat. Rev. Neurosci. 9, 839–855.
Furube, E., Mannari, T., Morita, S., Nishikawa, K., Yoshida, A., Itoh, M., et al., 2014. VEGF-dependent and PDGF-dependent dynamic neurovascular reconstruction in the neurohypophysis of adult mice. J. Endocrinol. 222, 161–179.
Furube, E., Morita, M., Miyata, S., 2015. Characterization of neural stem cells and their progeny in the sensory circumventricular organs of adult mouse. Cell Tissue Res. 362, 347–365.
Furusho, M., Roulois, A.J., Franklin, R.J., Bansal, R., 2015. Fibroblast growth factor signaling in oligodendrocyte-lineage cells facilitates recovery of chronically demyelinated lesions but is redundant in acute lesions. Glia. 63, 1714–1728.
Gensert, J.M., Goldman, J.E., 1997. Endogenous progenitors remyelinate demyelinated axons in the adult CNS. Neuron. 19, 197–203.
Girolamo, F., Ferrara, G., Strippoli, M., Rizzi, M., Errede, M., Trojano, M., et al., 2011. Cerebral cortex demyelination and oligodendrocyte precursor response to experimental autoimmune encephalomyelitis. Neurobiol. Dis. 43, 678–689.
Gonzalez-Perez, O., Romero-Rodriguez, R., Soriano-Navarro, M., Garcia-Verdugo, J.M., Alvarez-Buylla, A., 2009. Epidermal growth factor induces the progeny of subventricular zone type B cells to migrate and differentiate into oligodendrocytes. Stem Cells 27, 2032–2043.
Guo, F., Maeda, Y., Ma, J., Delgado, M., Sohn, J., Miers, L., et al., 2011. Macroglial plasticity and the origins of reactive astroglia in experimental autoimmune encephalomyelitis. J. Neurosci. 31, 11914–11928.
Hanrahan, E.O., Heymach, J.V., 2007. Vascular endothelial growth factor receptor tyrosine kinase inhibitors vandetanib (ZD6474) and AZD2171 in lung cancer. Clin. Cancer Res. 13, s4617–s4622.
Harirchian, M.H., Tekieh, A.H., Modabbernia, A., Aghamollaii, V., Tafakhori, A., Ghaffarpour, M., et al., 2012. Serum and CSF PDGF-AA and FGF-2 in relapsing-remitting multiple sclerosis: a case-control study. Eur. J. Neurol. 19, 241–247.
Hayakawa, K., Pham, L.D., Som, A.T., Lee, B.J., Guo, S., Lo, E.H., et al., 2011. Vascular endothelial growth factor regulates the migration of oligodendrocyte precursor cells. J. Neurosci. 31, 10666–10670.
Hiratsuka, D., Furube, E., Taguchi, K., Tanaka, M., Morita, M., Miyata, S., 2018. Remyelination in the medulla oblongata of adult mouse brain during experimental autoimmune encephalomyelitis. J. Neuroimmunol. 319, 41–54.
Imayoshi, I., Ohtsuka, T., Metzger, D., Chambon, P., Kageyama, R., 2006. Temporal regulation of Cre recombinase activity in neural stem cells. Genesis. 44, 233–238.
Jafarzadeh, A., Nemati, M., 2018. Therapeutic potentials of ginger for treatment of multiple sclerosis: a review with emphasis on its immunomodulatory, anti-inflammatory and anti-oxidative properties. J. Neuroimmunol. 324, 54–75.
Kaplan, M.R., Meyer-Franke, A., Lambert, S., Bennett, V., Duncan, I.D., Levinson, S.R., et al., 1997. Induction of sodium channel clustering by oligodendrocytes. Nature. 386, 724–728.
Kataria, H., Alizadeh, A., Shahriary, G.M., Saboktakin Rizi, S., Henrie, R., Santhosh, K.T., et al., 2018. Neuregulin-1 promotes remyelination and fosters a pro-regenerative inflammatory response in focal demyelinating lesions of the spinal cord. Glia. 66, 538–561.
Kawamoto, S., Niwa, H., Tashiro, F., Sano, S., Kondoh, G., Takeda, J., et al., 2000. A novel reporter mouse strain that expresses enhanced green fluorescent protein upon Cre-mediated recombination. FEBS Lett. 470, 263–268.
Liptak, Z., Berger, A.M., Sampat, M.P., Charil, A., Felsovalyi, O., Healy, B.C., et al., 2008. Medulla oblongata volume: a biomarker of spinal cord damage and disability in multiple sclerosis. AJNR Am. J. Neuroradiol. 29, 1465–1470.
Martin, R., McFarland, H.F., McFarlin, D.E., 1992. Immunological aspects of demyelinating diseases. Annu. Rev. Immunol. 10, 153–187.
McTigue, D.M., Tripathi, R.B., 2008. The life, death, and replacement of oligodendrocytes in the adult CNS. J. Neurochem. 107, 1–19.
Menn, B., Garcia-Verdugo, J.M., Yaschine, C., Gonzalez-Perez, O., Rowitch, D., Alvarez-Buylla, A., 2006. Origin of oligodendrocytes in the subventricular zone of the adult brain. J. Neurosci. 26, 7907–7918.
Miyata, S., 2015. New aspects in fenestrated capillary and tissue dynamics in the sensory circumventricular organs of adult brains. Front. Neurosci. 9, 390.
Mori, F., Rossi, S., Piccinin, S., Motta, C., Mango, D., Kusayanagi, H., et al., 2013. Synaptic

plasticity and PDGF signaling defects underlie clinical progression in multiple sclerosis. J. Neurosci. 33, 19112–19119.
Mori, F., Kusayanagi, H., Nicoletti, C.G., Weiss, S., Marciani, M.G., Centonze, D., 2014. Cortical plasticity predicts recovery from relapse in multiple sclerosis. Mult. Scler. 20, 451–457.
Nait-Oumesmar, B., Decker, L., Lachapelle, F., Avellana-Adalid, V., Bachelin, C., Baron-Van Evercooren, A., 1999. Progenitor cells of the adult mouse subventricular zone proliferate, migrate and differentiate into oligodendrocytes after demyelination. Eur. J. Neurosci. 11, 4357–4366.
Nait-Oumesmar, B., Picard-Riera, N., Kerninon, C., Decker, L., Seilhean, D., Hoglinger, G.U., et al., 2007. Activation of the subventricular zone in multiple sclerosis: evidence for early glial progenitors. Proc. Natl. Acad. Sci. U. S. A. 104, 4694–4699.
Nakashima, I., Fujihara, K., Okita, N., Takase, S., Itoyama, Y., 1999. Clinical and MRI study of brain stem and cerebellar involvement in Japanese patients with multiple sclerosis. J. Neurol. Neurosurg. Psychiatry 67, 153–157.
Nakano, Y., Furube, E., Morita, S., Wanaka, A., Nakashima, T., Miyata, S., 2015. Astrocytic TLR4 expression and LPS-induced nuclear translocation of STAT3 in the sensory circumventricular organs of adult mouse brain. J. Neuroimmunol. 278, 144–158.
Okada, S., Nakamura, M., Katoh, H., Miyao, T., Shimazaki, T., Ishii, K., et al., 2006. Conditional ablation of Stat3 or Socs3 discloses a dual role for reactive astrocytes after spinal cord injury. Nat. Med. 12, 829–834.
Paxinos, G., Franklin, K.B.J., 2001. The mouse brain in stereotaxic coordinates. Academic Press, San Diego.
Peterson, L.K., Fujinami, R.S., 2007. Inflammation, demyelination, neurodegeneration and neuroprotection in the pathogenesis of multiple sclerosis. J. Neuroimmunol. 184, 37–44.
Picard-Riera, N., Decker, L., Delarasse, C., Goude, K., Nait-Oumesmar, B., Liblau, R., et al., 2002. Experimental autoimmune encephalomyelitis mobilizes neural progenitors from the subventricular zone to undergo oligodendrogenesis in adult mice. Proc. Natl. Acad. Sci. U. S. A. 99, 13211–13216.
Proescholdt, M.A., Jacobson, S., Tresser, N., Oldfield, E.H., Merrill, M.J., 2002. Vascular endothelial growth factor is expressed in multiple sclerosis plaques and can induce inflammatory lesions in experimental allergic encephalomyelitis rats. J. Neuropathol. Exp. Neurol. 61, 914–925.
Reich, D.S., 2017. Imag(in)ing multiple sclerosis: time to take better pictures. J. Neuroimmunol. 304, 72–80.
Rivers, L.E., Young, K.M., Rizzi, M., Jamen, F., Psachoulia, K., Wade, A., et al., 2008. PDGFRA/NG2 glia generate myelinating oligodendrocytes and piriform projection neurons in adult mice. Nat. Neurosci. 11, 1392–1401.
Ruffini, F., Furlan, R., Poliani, P.L., Brambilla, E., Marconi, P.C., Bergami, A., et al., 2001. Fibroblast growth factor-II gene therapy reverts the clinical course and the pathological signs of chronic experimental autoimmune encephalomyelitis in C57BL/6 mice. Gene Ther. 8, 1207–1213.
Schmitt, C., Strazielle, N., Ghersi-Egea, J.F., 2012. Brain leukocyte infiltration initiated by peripheral inflammation or experimental autoimmune encephalomyelitis occurs through pathways connected to the CSF-filled compartments of the forebrain and midbrain. J. Neuroinflammation 9, 187.
Scolding, N., Franklin, R., Stevens, S., Heldin, C.H., Compston, A., Newcombe, J., 1998. Oligodendrocyte progenitors are present in the normal adult human CNS and in the lesions of multiple sclerosis. Brain. 121, 2221–2228 Pt 12.
Tsai, H.H., Niu, J., Munji, R., Davalos, D., Chang, J., Zhang, H., et al., 2016. Oligodendrocyte precursors migrate along vasculature in the developing nervous system. Science. 351, 379–384.
Wedge, S.R., Kendrew, J., Hennequin, L.F., Valentine, P.J., Barry, S.T., Brave, S.R., et al., 2005. AZD2171: a highly potent, orally bioavailable, vascular endothelial growth factor receptor-2 tyrosine kinase inhibitor for the treatment of cancer. Cancer Res. 65, 4389–4400.
Woodruff, R.H., Fruttiger, M., Richardson, W.D., Franklin, R.J., 2004. Platelet-derived growth factor regulates oligodendrocyte progenitor numbers in adult CNS and their response following CNS demyelination. Mol. Cell. Neurosci. 25, 252–262.
Yao, Z.F., Wang, Y., Lin, Y.H., Wu, Y., Zhu, A.Y., Wang, R., et al., 2017. Transplantation of PDGF-AA-overexpressing oligodendrocyte precursor cells promotes recovery in rat following spinal cord injury. Front. Cell. Neurosci. 11, 79.